Engineering Structures 312 (2024) 118196

Contents lists available at ScienceDirect

Engineering Structures

journal homepage: www.elsevier.com/locate/engstruct

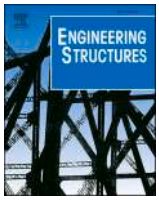

Influence of geotextile soil reinforcement layout on the deformation of a model soil-steel composite structure

Alemu Mosisa Legese [a,b,1], Adam Wysokowski [c,*,2], Adrian Różański [a,3], Maciej Sobótka [a,4]

[a] Faculty of Civil Engineering, Wroclaw University of Science and Technology, Poland
[b] Faculty of Civil and Environmental Engineering, Jimma Institute of Technology, Jimma University, Jimma P.O. Box 378, Ethiopia
[c] Institute of Building Engineering, University of Zielona Góra, Poland

ARTICLE INFO

Keywords:
Displacements
Double and single-layer geotextile
Geotextile reinforcement
Layout of reinforcement
Soil-steel composite structures

ABSTRACT

Geotextiles have become a subject of scientific research in recent years due to their ability to reduce pressure on soil masses and buried structures. However, the effective optimal of geotextiles above the crown of the shell of a soil-steel composite structure (SSCS) is not well described in the literature. This article presents an analysis of the impact of geotextile placement at different locations in the ground cover over the crown of the shell on the behaviour of the steel shell. The tests were carried out under different static loads. In the article, a comparative analysis of the results obtained on a natural scale with those obtained using the finite element method (FEM) is presented. For the purpose of the analysis, an experimentally verified computational model was developed and implemented in the commercial FE code, namely, the Zsoil numerical programme. The result demonstrated a significant reduction in maximum displacements and stresses upon employing a single-layer geotextile. The most significant reduction in vertical displacement, amounting to 37%, was observed when the geotextile was positioned at a shallower depth, closer to the load's zone of influence. Furthermore, it was found that vertical displacements in the crown can be reduced by up to 40% with the application of a double layer of geotextile. Furthermore, analysis of the effect of the position of the geotextile layer revealed that reinforcement is more effective when placed at a shallower depth, closer to the zone of influence of the load. These findings provide valuable information for designers who want to optimise geotextile placement for enhanced performance in SSCS designs.

1. Introduction

Soil-steel composite structures (SSCSs), made of steel plates (flat or corrugated) that cooperate with the backfill soil, have been widely used in culverts, bridges, tunnels, animal overpasses, etc. Recently, this type of structure has become increasingly popular due to its ease and rapid assembly, lower costs, shorter construction period, minimal or no maintenance requirements, reduced material usage (steel and soil), and environmental friendliness compared to traditional structures [1,2].

An increasing number of flexible steel plates with different shapes and geometries are being successfully used in various applications such as bridges, culverts, tunnels, and others [3–6].

There has been extensive research on the response of soil-steel composite structures to different loading conditions. Accordingly, the behaviour of SSCSs under static [7–12], semi-static, and dynamic loads [13–16], the response to seismic excitation [17–19], and the performance of SSCS under extreme loading [1,20–22], i.e., loading until failure were investigated based on field measurement or numerical simulation.

A substantial portion of the load-bearing capacity and stiffness of these types of structure is through interaction with the backfill. This indicates that the quality of the surrounding backfill will determine the performance of this structure under external load [2]. Since the soil is weak against tensile stress, it is important to improve the bearing

* Corresponding author.
E-mail address: awysokowski@infra-kom.eu (A. Wysokowski).
[1] ORCID:0000–0001-6420–6284
[2] ORCID:0000–0002-4547–2453
[3] ORCID:0000–0003-3150–6429
[4] ORCID:0000–0001-5166–9060

https://doi.org/10.1016/j.engstruct.2024.118196
Received 26 September 2023; Received in revised form 22 April 2024; Accepted 12 May 2024
Available online 23 May 2024

capacity of the soil in order to improve its stability by reducing the lateral displacement and settlement under different loading conditions. Adding a layer of geosynthetics to the backfill can significantly increase the stiffness of the composite structure. Thus, stress and displacement in the shell can be reduced [23–28].

In many cases, adhering to the minimum height of soil cover recommended by design standards at the crown of the shell is challenging due to natural factors, such as topographic conditions. These factors can make it technical and economically demanding to raise the road or railway embankment to meet the required specifications. There are several methods to overcome such difficulties and increase the bearing capacity of SSCSs [29–33]. Among the methods, additional structural elements that will distribute the external loads in larger areas by reducing direct pressure on the shell are frequently used. This additional element is often placed in the soil cover layer above the crown of the shell, with the purpose of reducing the internal forces acting on the shell [31]. This additional element can be reinforced concrete slab [31–33], which are widely used, or a reinforcing the backfill with geomembrane [29,34–36]. According to [36], comparing these two solutions, i.e., reinforced concrete slab and geomembrane, particularly in terms of cost, the second option (geomembrane) is found to be more feasible. Additionally, reinforcing soil using geomembrane materials is considered one of the most efficient method available for enhancing soil strength while reducing costs compared to traditional designs [37].

Thus, geotextiles have become a subject of scientific research in recent years. Moreover, they have gained widespread use as reinforcements in stabilizing various engineering structures, including footing, slopes, embankments, retaining walls, culverts, buried structures, and road construction over poor soils [24,38,39].

The effect of the geomembrane on the behaviour of SSCS is evaluated at field tests [29,36,37,40] and numerical simulations [29,41]. Wysokowski [36] conducted a full-scale test and investigated the influence of single-layer geotextile on the mechanical behaviour of SSCS subjected to different types of static loads. A single layer of geotextile contributes to reducing displacement and stresses in the shell. Furthermore, the vertical displacement in the crown of the shell was reduced by 30% and a slight stress reduction was observed. In their numerical simulation of a box-type SSCS with a 3.55 m span, Maleska et al. [41] analyzed a corrugated steel plate measuring 150 × 50 × 5 mm under a static load of 800 kN. In their model, a single-layer geotextile with thickness of 4.2 mm was placed in the middle of the height of the soil cover above the crown of the shell. The authors observed a redistribution of the applied load over the shell due to the use of a geomembrane above the SSCS shell. Furthermore, the application of geotextile resulted in a notable 28% reduction in vertical displacement at the crown of the shell compared to the model without geotextile reinforcement. EL-Sakhawy et al. [40] conducted a numerical simulation to investigate the effect of geogrids in a soil-steel culvert. Their analysis showed that the bending moment in the corrugated steel plate is significantly reduced. Bathurst et al. [34] analyzed the geocell-reinforced large-span SSCSs. From their analysis, they observed that thinner layers of geocell-reinforced soil height of cover could be used to provide the same or enhanced load-deflection response the same as a 1 m thick unreinforced soil cover. Vaslestad et al. [42] conducted full-scale test on geogrid reinforced corrugated steel box culvert. The maximum deflection of the geogrid reinforced shell subjected to static traffic load was reduced with 29.5%. Furthermore, the deflection at the crown of the shell was reduced by 17.8% under dynamic load. Hedge and Sitharam [43] evaluate the efficacy of geocell reinforcement in protecting buried pipelines, based on laboratory tests and the numerical model with a specific focus on reducing deformation and strain on PVC pipes under vehicle tire contact pressure. The primary findings revealed that the use of geocells led to a significant reduction in pipe deformation compared to alternative reinforcement methods.

Jeyapalan, and Lytton [44] conducted a numerical simulation on geosynthetics reinforced box culvert. The analysis showed that the vertical displacement at the crown of the shell was reduced by 30% for the geosynthetics-reinforced culvert. Dai, et al. [29], study the behavior of geotextile reinforced buried SSCS subjected to live loads. Results indicate that the application of live loads causes asymmetric deformation of the buried arch culvert. The amplitude of the culvert crown defection increases significantly as the vehicle gets closer to the crown of the shell.

The effect was analysed within the serviceability limit state in laboratory testing and numerical simulation. Few works [36,42] investigate the behaviour of membrane-reinforced SSCS under load beyond service load. Furthermore, limited study is available on the effect of a geotextile on the behaviour of SSCS during the construction stage.

Limited research is available on the effect of placing a single layer of geotextile at different positions above the crown of the shell. Therefore, the main objective of this study is to analyse the influence of placing a geotextile at different positions within the soil cover above the crown of the shell on the mechanical behaviour of SSCSs subjected to different static loads. In addition, the study examines the impact of using a double layer of geotextile. For the analysis, an experimentally validated computational model was developed using the commercial FE code, namely, the Zsoil numerical programme. The current work is the continuation of the full-scale test conducted by Wysokowski [36], who is co-author of current study.

2. The tested soil-steel structure details

The laboratory test conducted in full scale by Wysokowski [36] on soil-steel composite structure is used to validate the numerical simulation. The structure had the following dimensions: a span of 3.55 m, length of 13.7 m, rise of 1.42 m and soil cover of 0.6 m. The shell was assembled using corrugated profiles with a commercial designation, specifically the multiplate 150 mm × 50 mm (pitch x depth), and it had a thickness of 5.0 mm. The structure was reinforced with special ribs made of corrugated steel plates at the top section of the perimeter at the crown, with a width of 1.54 m. The corrugated steel plates were joined with 20 mm diameter bolts, having a minimum tensile strength of 830 MPa. For the backfill material, a well-graded soil with a maximum grain size of 32 mm was utilized. The backfill material used was well-graded soil with a maximum grain size of 32 mm. It was placed in nine layers with a maximum thickness of 20–30 cm and compacted to achieve a degree of compaction equivalent to 97% of the Standard Proctor test.

The test was primarily designed to assess the behaviour of the SSCS under specific load conditions in two distinct stages. Initially, the structure underwent testing without the inclusion of geotextile material. Subsequently, in the second stage of the testing, a single layer of geotextile material was introduced at the centre of the soil cover to observe its impact on the behaviour of the structure, as shown in Fig. 1. To determine the displacements and stresses in the steel structure, inductive gauges and strain gauges were installed on the inside surface of the culvert. During the backfilling stage, deformations and strains of the steel structure were measured. Once the backfilling was completed, a vertical load of 1512 kN was applied to the structure to assess the influence of the geotextile on its bearing capacity.

Analysis of test results revealed a notable difference in displacements and internal forces between the reinforced and unreinforced structure. On examining the data from both stages of the test, it became evident that the inclusion of a geotextile in the backfill layer led to a reduction in displacements of the corrugated steel structures tested by as much as 30%. Furthermore, when comparing stress values at the crown of the structure, a slight reduction was observed under maximum static loads. The reduction in displacement and stress observed when using geotextile is attributed to the phenomenon of redistribution of the applied load over a larger area of the corrugated steel structure as it undergoes subsequent loading. Such behavior demonstrates the interaction of the soil with the corrugated steel structure, as evidenced by previous studies [38,45].

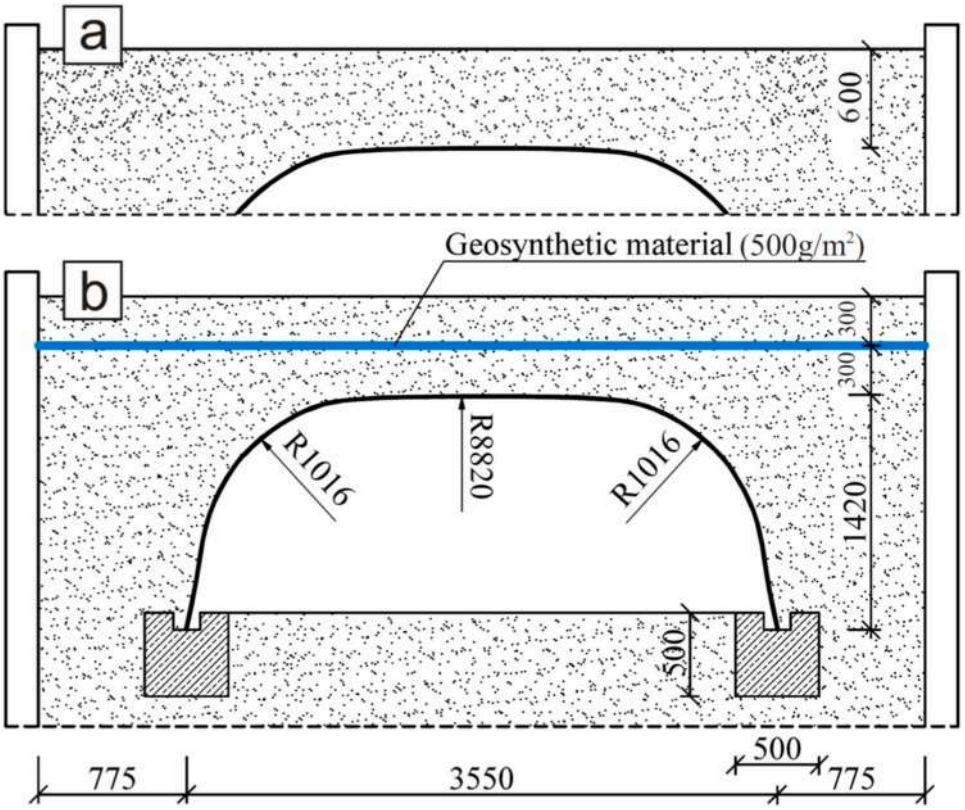

Fig. 1. Cross-section of the soil steel composite structure in laboratory test: a) without reinforcement, b) with geotextile[36].

The purpose of the research described in this article is to verify numerically the tests performed on a full scale. Furthermore, the objective of the research was to check the effect of the reinforcement system on the geometric parameters of the steel shell, which would have been a very expensive undertaking in the case of full-scale tests.

3. Numerical modelling

The commercial FE code, namely, Zsoil software programme [46], based on FEM, was used for the numerical analysis of the soil-steel composite structure. This FE code allows us to utilize its capabilities effectively for the numerical analysis required for our study. In particular the program offers constitutive models typically used for soil and stage-wise simulation, reflecting credibly the plastic behaviour of the backfill. The shell was modeled as a 2D object in plane strain using beam elements for the shell structure and solid elements for the soil (backfill) medium (Fig. 2).

The connection between the shell and the foundation was assumed to be pinned with fixed displacement in both directions and free in rotation. To account for second-order effects, the large deformation mode is

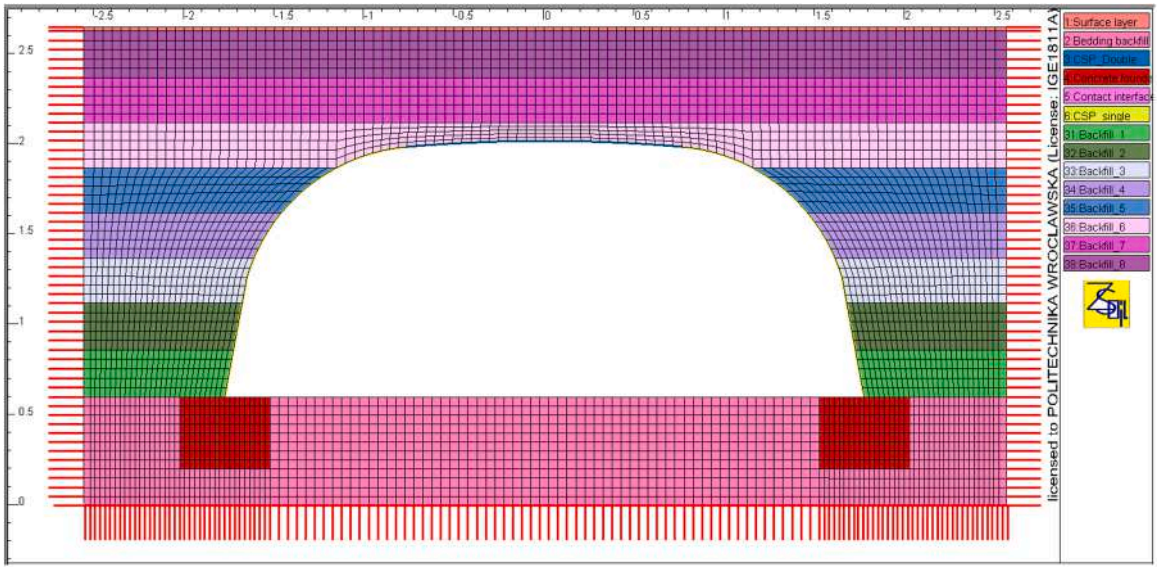

Fig. 2. Geometry and finite element mesh adopted in the numerical model.

activated. Furthermore, a mesh size sensitivity analysis was performed to ensure that the results are not influenced by the element size. Finally, a fine mesh size of 5 cm was used for both the shell and the surrounding backfill. In terms of boundary conditions, the vertical edges of the domain were restrained against horizontal displacements, and the bottom boundary was fixed in all directions.

3.1. Parameters of the materials

3.1.1. Corrugated steel plate

The corrugated steel plate (CSP) was modelled using two-dimensional nonlinear beam elements, employing an elastic-perfectly plastic constitutive relation. It is also assumed to be continuous in the out-of-plane Z direction, following the considerations presented in previous works [47–49]. In the crown section, the structure was mounted by double corrugated sheets (See Fig. 3b) and the other section of the structure was single corrugation. To reflect this effect in simulation, section parameters of the shell are calculated separately for both double and single corrugation and included in the model.

The parameters of the shallow corrugation (multi-plate) used in the test adopted in this work is based on the manufacturer catalog [50] that for the single corrugation (without stiffening rib). Accordingly, the cross-sectional area and moment of inertia for a single corrugation are 6.30 mm^2/mm and 1978 mm^4/mm respectively. For a two-layer shell (with stiffening rib), the corresponding values are 0.0126 mm^2/mm and 13,485 mm^4/mm.

In the model, the CSP was characterised by parameters specified in the European Standard EN 10025. These parameters include a minimum plate yield stress of 250 MPa, Young's modulus of 210 GPa, and a tensile strength of 270 MPa.

3.1.2. Backfill

The elastic-perfectly plastic constitutive model with Coulomb-Mohr yield criterion is assumed for the backfill soil; the unassociated plastic flow rule is prescribed, and it was described by a dilatancy angle determined based on the ZSoil user manual [46]:

$$\psi = \max\left(0.1\varphi, \varphi - 25^{\circ}\right) \tag{1}$$

where ψ is the dilatancy angle and φ the angle of internal friction.

The material parameters used in the computations are shown in Table 1. To avoid a premature calculation termination caused by soil failure under ultimate load and to ensure the numerical stability of the model, the cohesion value was increased.

Numerical simulations were conducted, considering the construction stages of backfill. To replicate the field measurement, stage constructions were taken into account. In addition, each layer was subjected to a surface load of 50 kPa to simulate the load associated with the actual soil compaction process. The geometry of the model was described in Fig. 1.

Table 1
The material parameters used in the computations.

Corrugated steel plate		Backfill
Young's modulus (MPa)	205,000	60
Tensile strength (MPa)	270	-
Yield limit (MPa)	250	-
Poisson ratio	0.3	0.15
Unit weight (kN/m^3)	78.6	19
Cohesion (kPa)	-	12
Friction angle (°)	-	36
Dilatancy angle (°)	-	11

3.1.3. Contact interface

The frictional interface between the shell elements and the backfill was assumed. This means that the soil medium separates from the shell if the shell moves away from the backfill material, and subsequent contact renewal is allowed when the shell and backfill material come close together again. The behaviour of the contact interface was described using the Coulomb condition. The plastic slip was governed by a non-associated plastic flow rule with the dilation angle value set to y = 0. The Coulomb condition governs the value of the maximum tangential stress in contact elements:

$$|\tau_f| \leq a + \sigma \tan \delta \tag{2}$$

Where adhesion a = 0, the internal angle of friction δ = 0.6, $\varphi \approx 22^{\circ}$ and $\varphi = 36^{\circ}$, is the internal angle of friction of the adjacent soil. The dilation angle was adopted as y = 0°. Elastic deformation moduli (normal and tangential stiffness) for interface elements were determined in accordance with Zsoil Users' Manual [46] as:

$$Kn \approx K_t = E/h \tag{3}$$

Where E is its modulus of elasticity of the weakest adjacent material, h is the depth of the very thin weak layer (interface). Based on Eq. 3, the value of normal and tangential stiffness adopted in the calculation was 1.0e^6 kN/m^3, while 8.0e^4 kN/m^3 for the interface between the geotextile and the backfill. Similar assumption is considered in the work of [41].

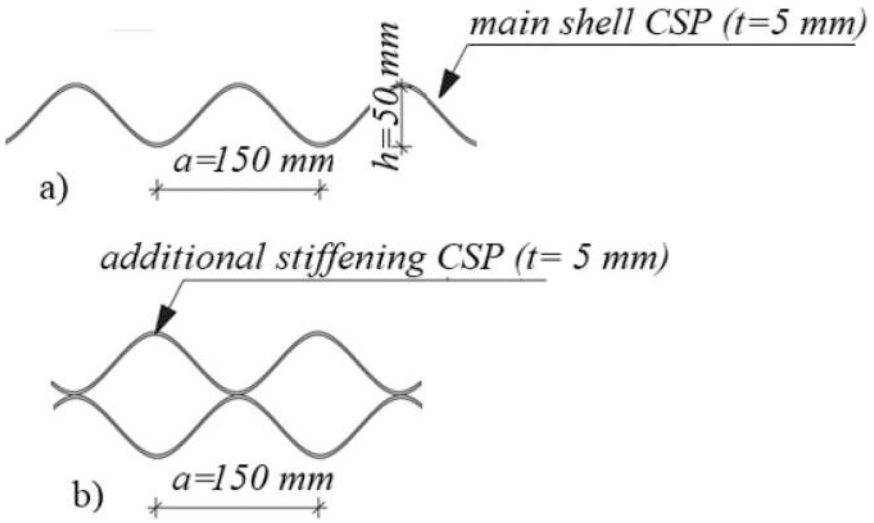

Fig. 3. Corrugated steel profiles: a) main shell, b) main shell with stiffening rib.

3.1.4. Reinforcing geotextile

The geotextile is modelled as a non-linear truss element, assuming elastic-perfectly plastic behaviour with limited tensile stress and the prestressing effect is also taken into consideration. In our current model, the prestress of around 6% of the tensile strength of the geotextile material is considered. This approach is similar to the method used in Alfaro et al., [51], where a prestress of 3.5% of the geotextile's tensile strength was considered. The tensile strength of geotextile in the model is 3.4 MPa with zero compressive strength and a thickness of 4.2 mm.

As shown in Fig. 4(a–e), a single layer of geotextile is placed at five different positions above the crown of the shell. Additionally, another model is prepared by placing two layers of geotextile at different positions, as illustrated in Fig. 4(f). A summary of the models and their respective locations is presented in Table 2.

3.2. Model validation

The validation process was carried out by comparing the measured and calculated results during the construction process. The results of displacement during the construction stage are compared and presented.

Table 2
Position of the geotextile in the soil above the crown of the shell.

Model	The Position of the Geotextile
Reference	Without geotextile
Model-I	0.1 m above the crown of the shell
Model-II	0.2 m above the crown of the shell
Model-III	0.3 m above the crown of the shell
Model-IV	0.4 m above the crown of the shell
Model-V	0.5 m above the crown of the shell
Model-VI	0.1 m and 0.3 m above the crown of the shell

3.2.1. Analysis during the construction stage

The 2D analyses were performed step by step, starting with placing the shell on 0.50 m × 0.50 m concrete footing with backfilling. After placing each backfill layer, a compaction load, which was related to the actual soil compaction process, was simulated as a surface load. This compaction load is symmetrical with respect to the vertical axis of the structure. The compaction load at a fifth layer of the model is shown in Fig. 5. Once the final layer of fill has been placed over the top of the structure, loads are applied to simulate the behaviour of the structure

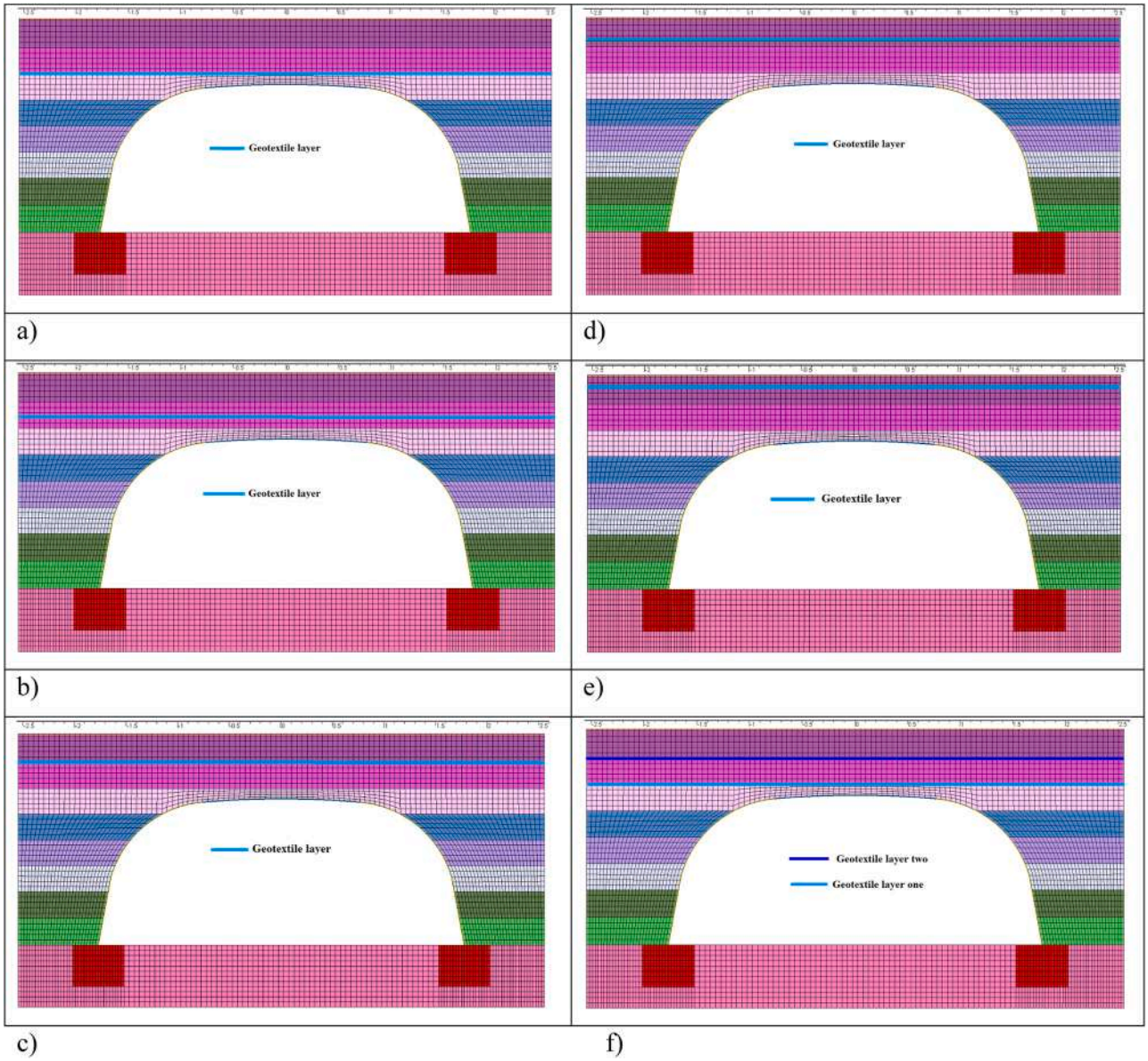

Fig. 4. Position of geotextile: a) Model I, b) Model II, c) Model III, d) Model IV, e) Model V, f) Model VI.

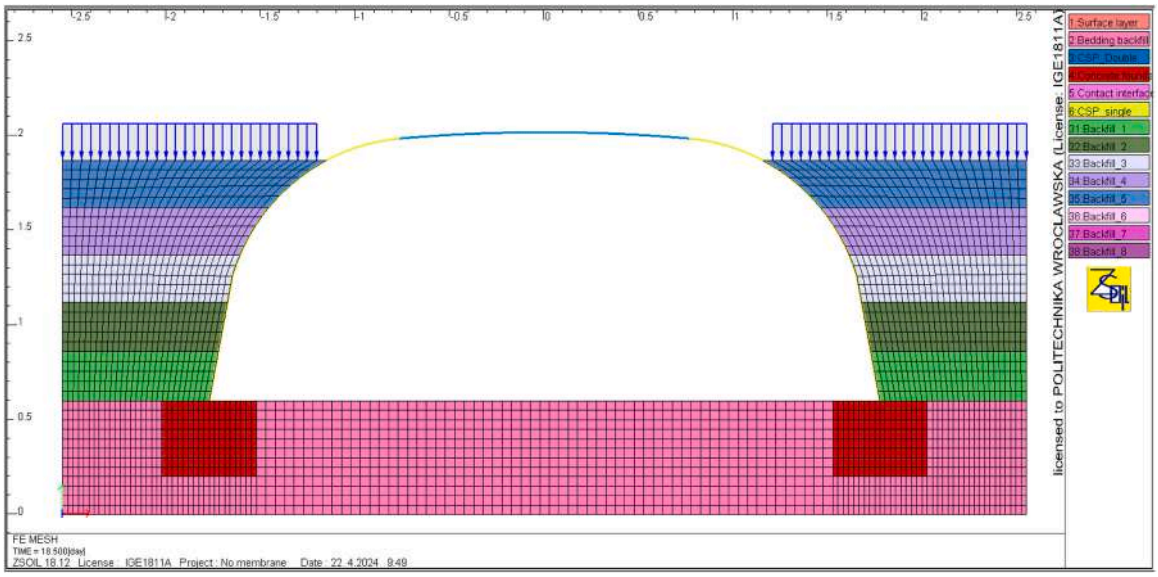

Fig. 5. Backfill and compaction load in the fifth layer of the model.

under different static loads, including the ultimate load.

According to [47], the effect of shell prestressing can be reproduced by taking into account staged backfilling. This will help to reproduce the real behaviour of the structure under different loading conditions.

To capture the deformation of the shell, field measurements were recorded during backfilling using a set of strain gauges attached to the circumference of the middle section of the CSP. The measured displacement at the crown of the structure is considered to validate the numerical simulation during the construction stage. As shown in Fig. 6, the numerical modelling results are in close agreement with the field measurements for the crown deformation of the CSP. The numerical model predicts a maximum downward movement of around − 1.70 mm when the backfill reaches the last stage and assumes a model of pavement level, whereas the field measurement recorded − 1.89 mm. As observed from field measurements and the FEM model, the values and signs of displacements undergo a change as the number of layers increases. The FE model accurately determines displacements within the shell during the construction stage. However, it slightly underestimates the peak displacement (both upward and downward), deviating by approximately 11% from the field measurements. Moreover, in the model, the crown of the shell initially exhibited upward deflection as the backfilling process progressed, and this upward deflection continued until the backfill reached layer five. Subsequently, as the backfilling process extended beyond layer five, the crown of the shell started moving downward. The maximum upward and downward vertical displacement of the shell during construction were less than 0.1% of the structure rise, which is in agreement with the requirements of CHBDC (CSA 2019) [52] code limit of 2%.

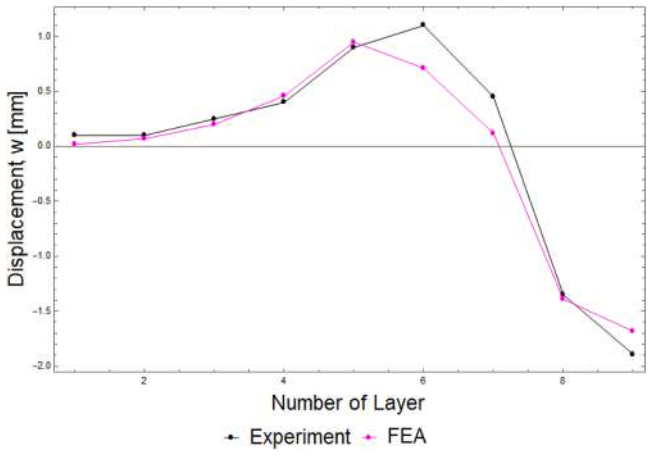

Fig. 6. Comparison of measurements and numerical modeling results for the crown deformation during backfilling.

4. Result and discussion

4.1. Effect of geotextile at construction stages

The presented numerical model demonstrates that the behaviour of the shell structures during the backfilling process is complex. As the number of layers increases, the displacement values and signs change. This finding is consistent with the results of Korusiewicz and Kunecki [53], who conducted a full-scale test to investigate the mechanical behaviour of the SSCS during backfilling. Furthermore, in the numerical model, when the single layer of geotextile was placed at the center of the depth of soil cover, the vertical displacement during backfill was reduced by 22% (see Fig. 7). The maximum reduction in vertical displacement occurred when the geotextile was placed at a shallower depth (closer to the zone of influence of the load), specifically at 0.5 m above the crown of the shell, where the reduction reached 37%.

Following the investigation of the impact of a single layer of geotextile on the deformation behaviour of the shell during the backfilling and compaction process, the study continues to examine the effects of positioning two layers of geotextile at varying locations. In Model-VI (depicted in Fig. 4(f)), one layer of geotextile is strategically positioned 0.1 m above the crown of the shell, while the second layer is situated at the soil cover's center, precisely 0.3 m above the crown of the shell. This configuration aims to evaluate the influence of dual reinforcement on the shell's deformation behaviour, which is subsequently analysed and visualised in Fig. 8.

When the geotextile layer is doubled, a significant improvement in structural performance is achieved. As shown in Fig. 8, there is a notable 40% reduction in vertical displacement compared to the unreinforced structure. Additionally, compared to the single-layer reinforcement scenario, a substantial 22% reduction in vertical displacement is still observed. These findings emphasize the effectiveness of employing a dual-layer geotextile reinforcement strategy for enhancing structural stability.

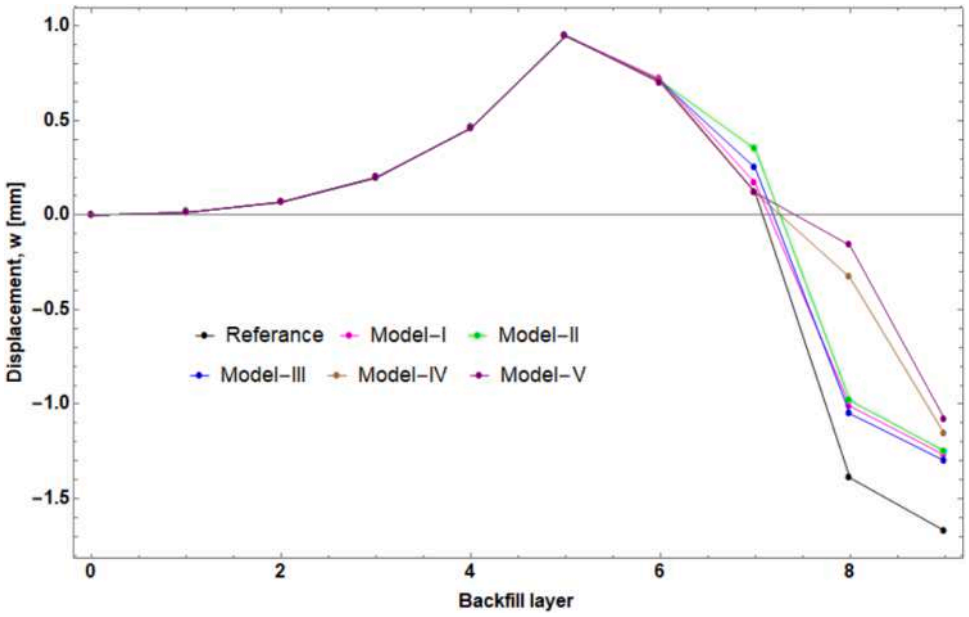

Fig. 7. Vertical displacement at the crown of the shell during backfilling by placing geotextile at deferent position above the crown of the shell.

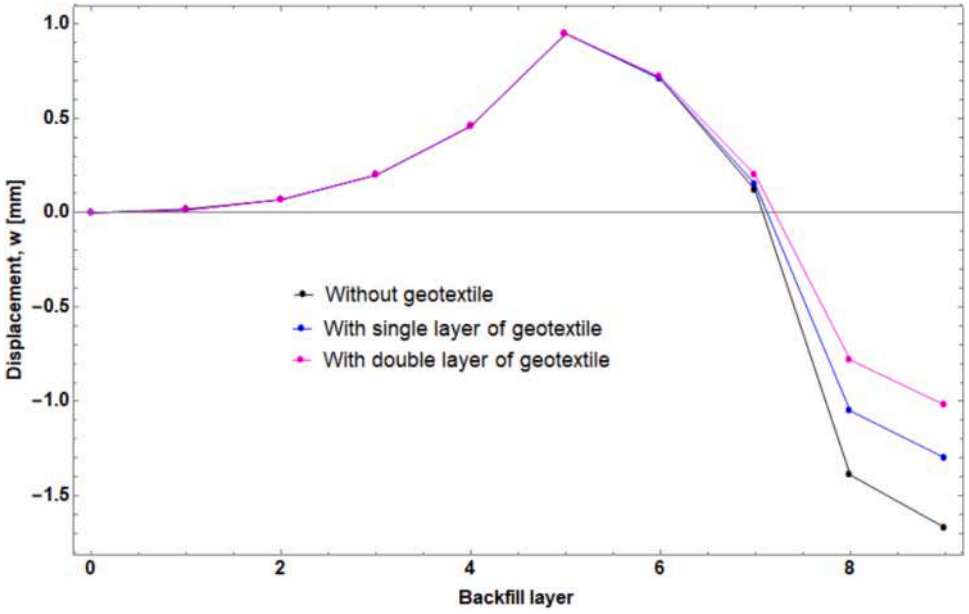

Fig. 8. Effect of double geotextile on the vertical displacement of the shell at the crown during backfilling.

4.2. Effect of the geotextile in the structure subjected to external load

The box-type structure is simulated under the load of 1512 kN, similar to the condition of the full-scale test. In this simulation, a single layer of geotextile is placed at five different positions within the soil above the height of the soil cover. As shown in Fig. 9, the maximum vertical displacement at the crown of the shell is reduced in the range of 17 to 21% with single-layer geotextile at different positions. The most significant reduction is observed when the geotextile is placed near the top of the soil cover or in close proximity to the position where the load is applied, i.e., 0.5 m above the crown of the shell. This positioning effectively prevented the overstressing effect on the shell structure, leading to improved performance.

On the other hand, when the geotextile is placed at 0.1 m, which is close to the shell, the displacement decreases by 17%. This shows that geotextile is more effective when it is placed at a position far from the shell and nearby the loading surface. A similar finding was obtained by [34]. In their work, it was reported that the reinforcement is more effective when placed at shallower depths. The reduction in displacement is due to the advantage of geotextile in strengthening the backfill soil in such a way that the loads are distributed through the soil depth of cover over as the structure is subject to an external load.

In the case of stress values in shell at the crown of the structure, notable differences were observed between the reinforced and unreinforced structure. The maximum stress was reduced by 32% when reinforcement was employed. Similar to the displacemnt, this maximum reduction was observed when the reinforcement was placed near the top surface, specifically at position 5, as illustrated in Fig. 10. According to [36], when the backfill soil above the shell is reinforced with a single layer of geotextile, the stress in the shell of the soil steel structure can be

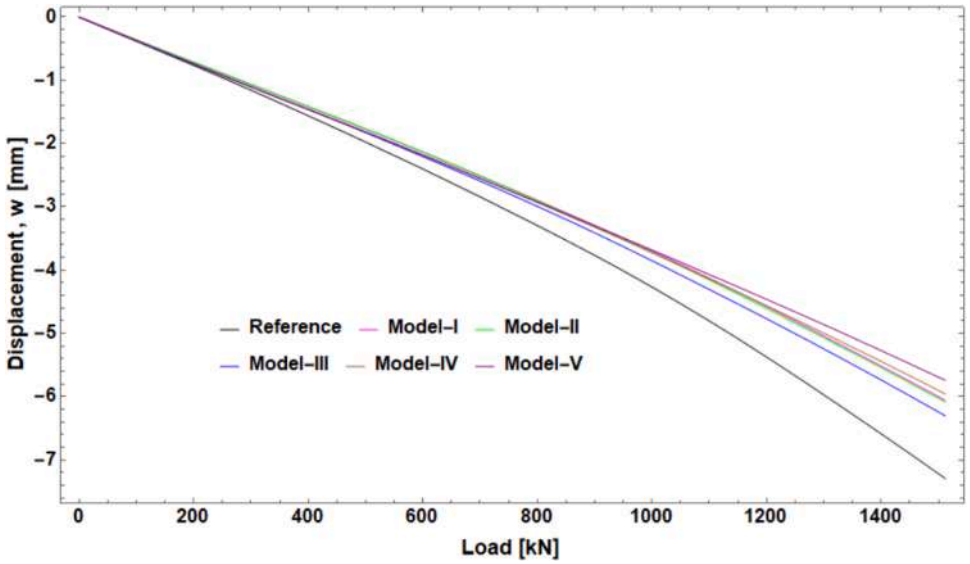

Fig. 9. Vertical displacement at the crown of the shell by placing single layer of geotextile at different positions.

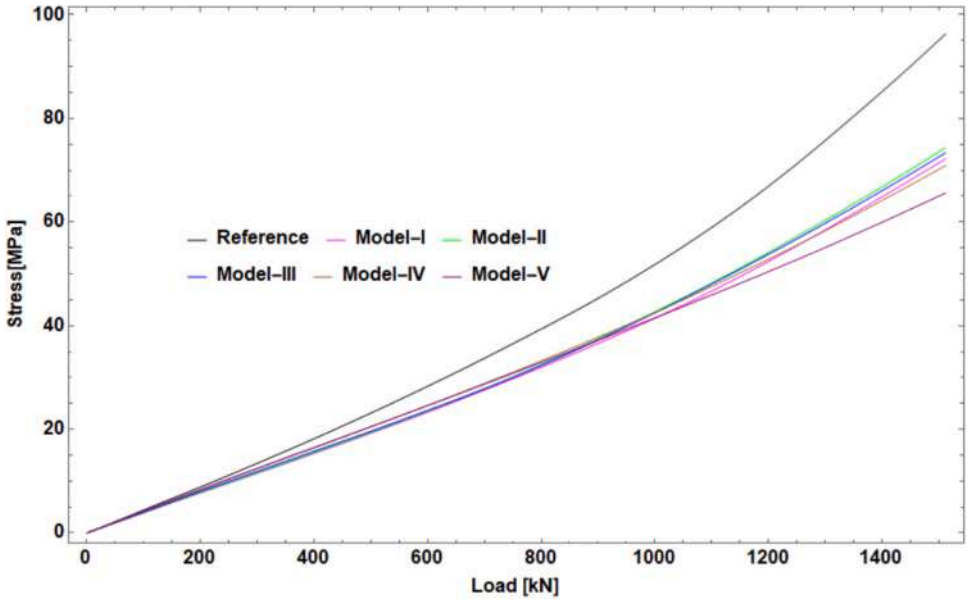

Fig. 10. Stresses at the crown of the shell by placing geotextile at different positions.

significantly reduced, with potential reductions of up to 40%.

The stress at the crown of the central shell, presented here as a numerical simulation result, was calculated based on Eq. (3):

$$\sigma_x = \frac{(N - N_0)}{A} + \frac{(M - M_0)}{I}\frac{h}{2} \tag{4}$$

where N, M stands for the axial force and the bending moment, respectively, and N_0 and M_0 are the values of the axial force and moment for the calculated structure at the start of the calculation, I and A are moment of inertia and the cross section area respectively. while h is the thickness of the steel shell.

4.3. Effect of double layer of geotextile

This model investigates the effect of reinforcing the structure with a double layer of geotextile. For the double geotextile reinforcement, the membranes were placed at the center (0.3 m above the crown of the shell) and 0.1 m above the crown. In the case of single layer of geotextile reinforcement, the geotextile was placed at the center, approximately 0.3 m above the crown of the shell. Compared with single layer of geotextile reinforcement, the vertical displacement at the crown of the shell is reduced by 11% when using double reinforcement as shown in Fig. 11.

Fig. 12 shows the distribution of the vertical deformation of the backfill surrounding the shell under applied load. It is evident that the unreinforced structure, as showed in Fig. 12(a), exhibits the highest deformation, whereas the scenario with a double layer of geotextile reinforcement, illustrated in Fig. 12(g), demonstrates the least deformation. This underscores the notable effectiveness of the geotextile reinforcement layer in mitigating vertical deformation within the backfill. In particular, when evaluating the impact of a single layer of geotextile, the greatest reduction in vertical soil deformation occurs when the reinforcement is positioned at shallower depths, as clearly evidenced in Fig. 11(f). Furthermore, the deformation of the backfill around the crown of the shell is significantly reduced with the use of

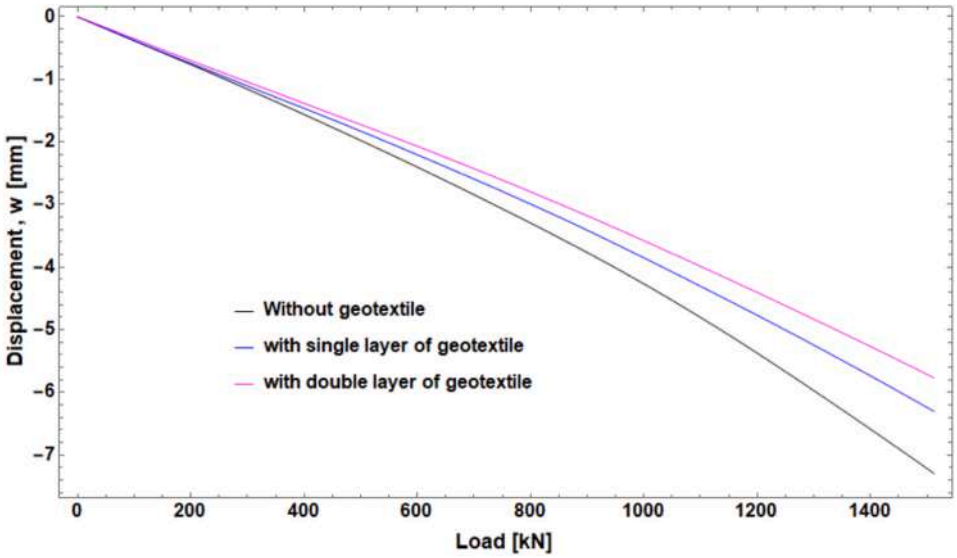

Fig. 11. The influence of single and double layer geotextile on vertical displacement of the shell at crown.

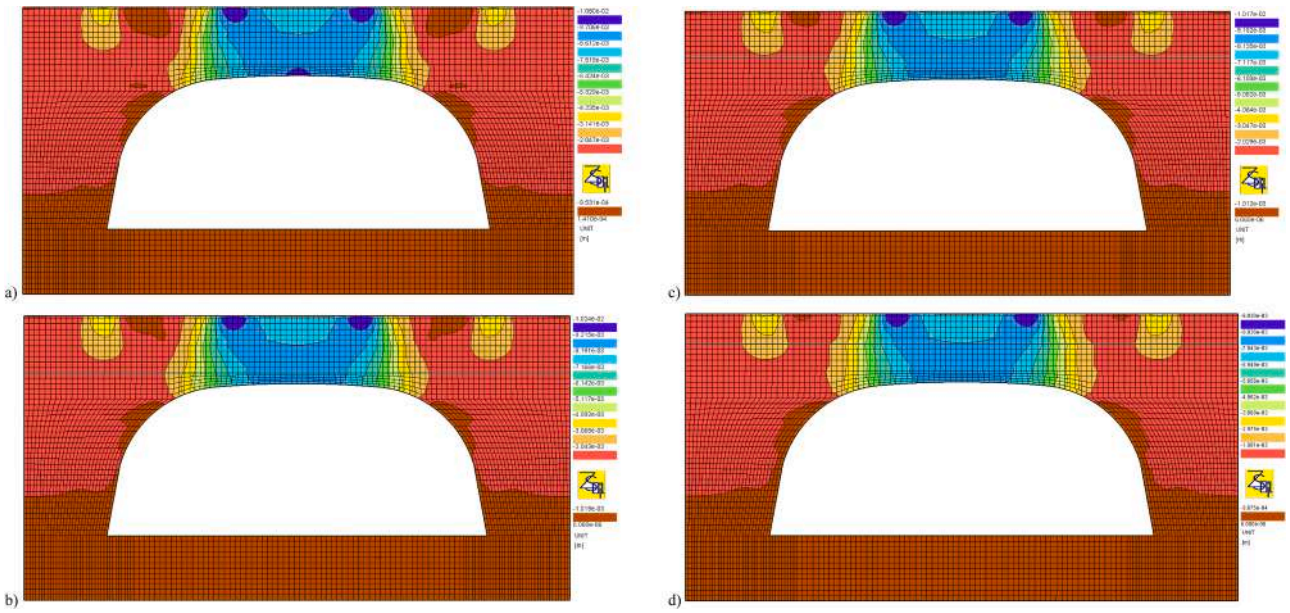

Fig. 12. Distribution of vertical deformation of the soil: a) unreinforced, b) reinforced (Model I), c) reinforced (Model II), d) reinforced (Model III), e) reinforced (Model IV), f) reinforced (Model V) g) double reinforced (Model VI).

geotextile. In general, the analysis reveals a significant reduction in deformation around the shell when the backfill is reinforced with geotextile.

5. Summary and conclusions

In conclusion, the results of the tests highlight the significant potential of geotextile applications in improving the structural stability of different systems. The use of a single-layer geotextile has shown a considerable reduction in maximum stresses and displacements, indicating its effectiveness in mitigating external forces' negative impacts. Furthermore, the use of a double layer of geotextile has demonstrated notable advantages, with a remarkable reduction of forty percent in vertical displacements within the crown.

The importance of geotextile placement has been emphasized through comprehensive analyses. These investigations have clearly indicated that the positioning of the geotextile layer profoundly influences its reinforcing capabilities. In particular, when placed at a shallower depth closer to the load's zone of influence, the geotextile's reinforcing effectiveness is more prominent. Among the main conclusions of the analyses, the following should be briefly highlighted:

- The results of the numerical simulation has good agreement with the full-scale test, proving that geotextile reinforcement can effectively decrease vertical displacements during construction stage and under external laod. Mover the stresses in the shell is also deacreased as well.
- The numerical simulation results demonstrate good agreement with the full-scale test, providing that geotextile reinforcement significantly reduces the vertical displacements during both construction

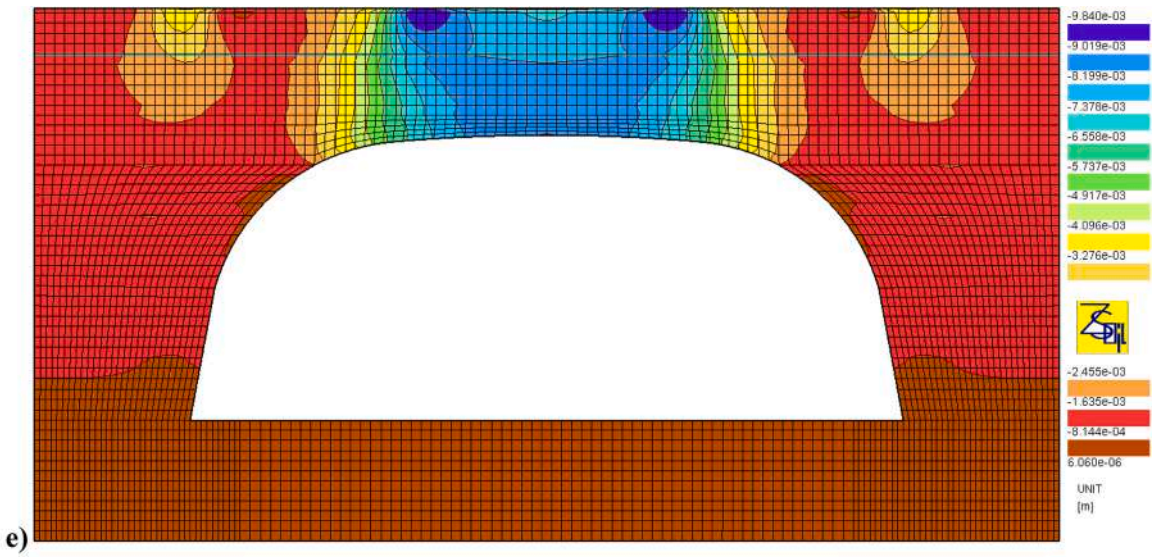

e)

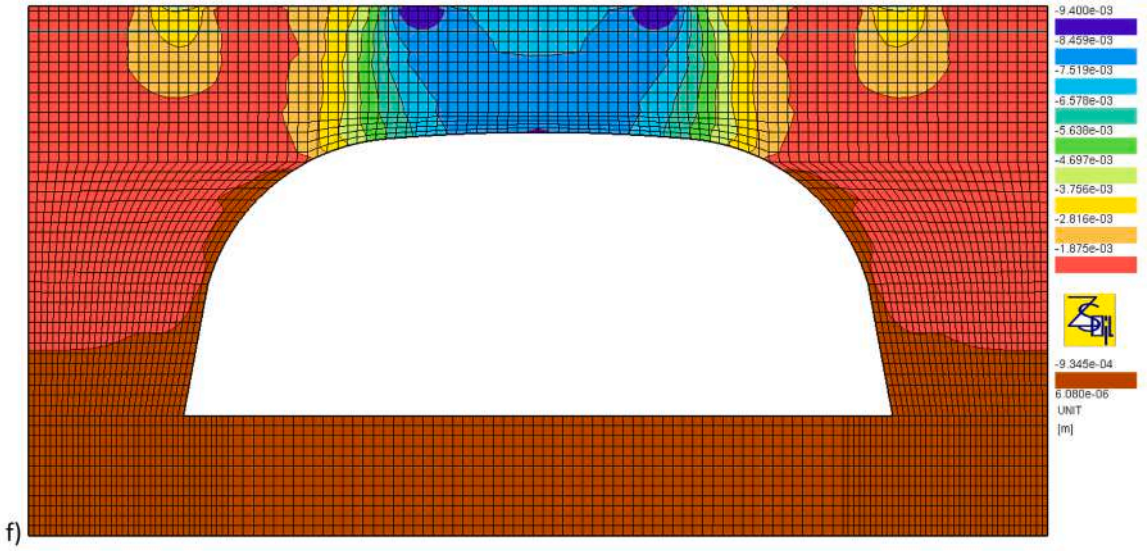

f)

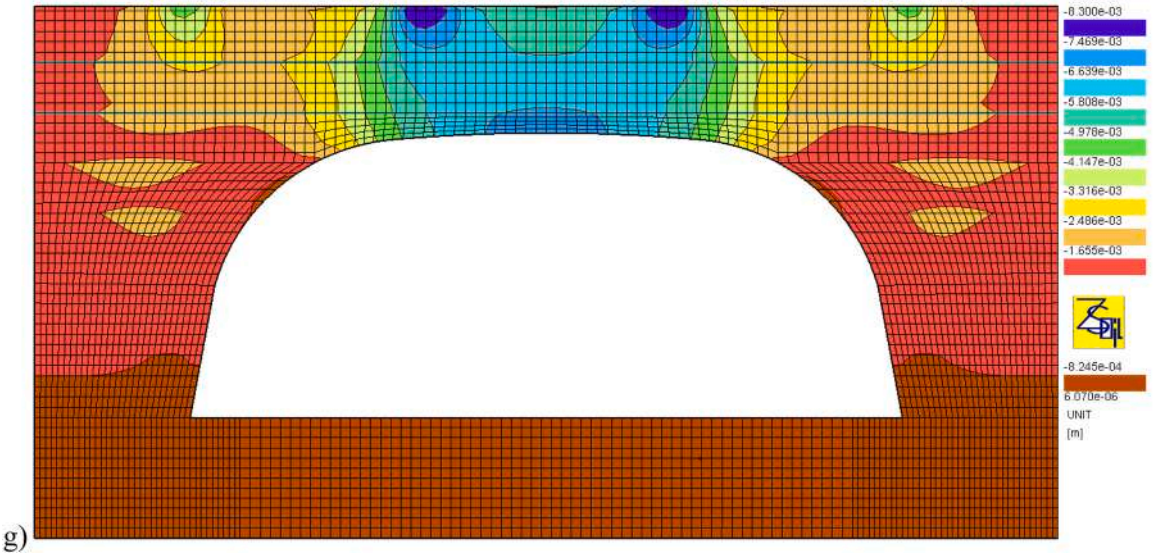

g)

Fig. 12. (*continued*).

stage and under external loads. Furthermore, this reinforcement strategy also contributes to a notable reduction in stresses within the shell.

- Placing a single layer of geotextile at the center of the soil cover depth resulted in a reduction of vertical displacement during backfilling by up to 22%. However, when the geotextile was positioned at a shallower depth, specifically at 0.5 m above the crown of the shell, the vertical displacement was reduced by 37%.
- A significant reduction in maximum stress and displacement values is observed using single-layer geotextile. This reduction in vertical displacement at the crown can reach to fory percent using a double layer of geotextile.
- Geotextile is more effective when it is placed at a position of shalower depth that is nearby the loading surface.
- The structure's load-bearing capacity is significantly improved using the reinforcement, and for economic purposes, a single layer is convenient by placing it at the appropriate position.
- Geotextile reinforcement significantly reduces vertical deformation in the backfill around the shell, particularly with a double layer or when positioned at shallower depths, showcasing its effectiveness in reducing deformation and enhancing structural stability.

These insights collectively emphasize the importance of thoughtful geotextile implementation in engineering and construction practices. By tailoring the placement and configuration of geotextile materials, designers and engineers can harness their potential to optimize structural performance and resilience. As we continue to explore innovative solutions for enhancing infrastructural sustainability, these findings offer a valuable roadmap for harnessing the benefits of geotextiles to create safer, more resilient systems that can withstand a wide range of environmental pressures and loading conditions.

CRediT authorship contribution statement

Alemu Mosisa LEGESE: Formal analysis, Software, Writing – original draft, Writing – review & editing. **Adam Wysokowski:** Supervision, Validation, Writing – review & editing. **Adrian RÓŻAŃSKI:** Supervision. **Maciej SOBÓTKA:** Supervision.

Declaration of Competing Interest

We wish to confirm that there are no known conflicts of interest associated with this publication and there has been no significant financial support for this work that could have influenced its outcome. We declare that I have no known competing financial interests or personal relationships that could have appeared to influence the work reported in this paper. We confirm that the manuscript has been read and approved and there are no other persons who satisfied the criteria for authorship but are not listed. We confirm that I have given due consideration to the protection of intellectual property associated with this work and that there are no impediments to publication, including the timing of publication, with respect to intellectual property. In so doing I confirm that I have followed the regulations of our institutions concerning intellectual property. We understand that the Corresponding Author is the sole contact for the Editorial process (including direct communications with the office).

Data availability

No data was used for the research described in the article.

References

[1] Wadi A, Pettersson L, Karoumi R. On predicting the ultimate capacity of a large-span soil–steel composite bridge. Int J Geosynth Gr Eng 2020;vol. 6(4):1–13. https://doi.org/10.1007/s40891-020-00232-z.

[2] Maleska T, Beben D. Numerical analysis of a soil-steel bridge during backfilling using various shell models. Eng Struct 2019;vol. 196(January):109358. https://doi.org/10.1016/j.engstruct.2019.109358.

[3] Pettersson L, Wadi A, Williams K. Structural design of flexible culverts development trends. Arch Inst Inżynierii Lądowej 2017;(April):237–50. https://doi.org/10.21008/j.1897-4007.2017.23.22.

[4] Legese AM, Sobótka M, Machelski C, Różański A. "Behaviour of soil-steel composite structures during construction and service: a review,". Arch Civ Eng 2023;vol. 69 (4):263–92. https://doi.org/10.24425/ace.2023.147659.

[5] Legese AM, Różański A, Sobótka M. Effect of shell spacing on mechanical behavior of multi-span soil-steel composite structure. Heliyon 2023;vol. 10(1):e23376. https://doi.org/10.1016/j.heliyon.2023.e23376.

[6] M. Sobótka, "Multi-scale numerical modeling of backfill-shell interaction in soil-shell structures (Polish)," Politechnika Wrocławska, 2016.

[7] Embaby K, El Naggar MH, El Sharnouby M. Performance of large-span arched soil–steel structures under soil loading. " *Thin-Walled Struct* Mar. 2022;vol. 172: 108884. https://doi.org/10.1016/J.TWS.2022.108884.

[8] Antoniszyn G, Machelski C, Michalski B. "Live load effects on a soil-steel bridge founded on elastic supports,". Stud Geotech Mech 2006;vol. Vol. 28(nr 2-4):65–82.

[9] Flener EB. Soil-steel interaction of long-span box culverts—performance during backfilling. J Geotech Geoenviron Eng 2010;vol. 136(6):823–32. https://doi.org/10.1061/(asce)gt.1943-5606.0000287.

[10] Sobótka M. Numerical simulation of hysteretic live load effect in a soil-steel bridge. Stud Geotech Mech 2014;vol. 36(1):104–10. https://doi.org/10.2478/sgem-2014-0012.

[11] Ezzeldin I, El Naggar H. Numerical modelling of induced stresses in buried corrugated metal structures due to compaction efforts. Transp Geotech 2022;vol. 32:100706. https://doi.org/10.1016/j.trgeo.2021.100706.

[12] Nakhostin E, Kenny S, Sivathayalan S. A numerical study of erosion void and corrosion effects on the performance of buried corrugated steel culverts. Eng Struct 2022;vol. 260:114217. https://doi.org/10.1016/j.engstruct.2022.114217.

[13] Bayoğlu Flener E, Karoumi R. Dynamic testing of a soil–steel composite railway bridge. Eng Struct Dec. 2009;vol. 31(12):2803–11. https://doi.org/10.1016/J.ENGSTRUCT.2009.07.028.

[14] Beben D. Experimental study on the dynamic impacts of service train loads on a corrugated steel plate culvert. J Bridg Eng 2013;vol. 18(4):339–46. https://doi.org/10.1061/(ASCE)BE.1943-5592.0000395.

[15] Yu S, et al. Experimental study on the elastic-plastic dynamic response of shallow-buried corrugated steel-plain concrete composite structures under long-duration plane blast wave loading. Eng Struct 2023;vol. 285:115986. https://doi.org/10.1016/j.engstruct.2023.115986.

[16] Mellat P, Andersson A, Pettersson L, Karoumi R. Dynamic behaviour of a short span soil–steel composite bridge for high-speed railways – Field measurements and FE-analysis. Eng Struct Jun. 2014;vol. 69:49–61. https://doi.org/10.1016/J.ENGSTRUCT.2014.03.004.

[17] Maleska T, Beben D. "Effect of the soil cover depth on the seismic response in a large-span thin-walled corrugated steel plate bridge,". Soil Dyn Earthq Eng 2023; vol. 166:107744.

[18] Maleska T, Beben D. Behaviour of corrugated steel plate bridge with high soil cover under seismic excitation. MATEC Web Conf 2018;vol. 174. https://doi.org/10.1051/matecconf/201817404003.

[19] Mahgoub A, El H. Naggar, "Assessment of the seismic provisions of the CHBDC for CSP culverts. *Int Conf GeoOttawa* 2017:1–4.

[20] Brachman RWI, Moore ID, Mak AC. Ultimate limit state of deep-corrugated large-span box culvert. Transp Res Rec 2010;vol. 2201(1):55–61. https://doi.org/10.3141/2201-07.

[21] Regier C, Hoult NA, Moore ID. "Laboratory study on the behavior of a horizontal-ellipse culvert during service and ultimate load testing,". J Bridg Eng 2017;vol. 22 (3):4016131.

[22] Wysokowski A. Full scale tests of various buried flexible structures under failure load. Sci Rep 2022;vol. 12(1):1–14. https://doi.org/10.1038/s41598-022-04969-7.

[23] Chen J-F, Guo X-P, Xue J-F, Guo P-H. Load behaviour of model strip footings on reinforced transparent soils. Geosynth Int 2019;vol. 26(3):251–60. https://doi.org/10.1680/jgein.19.00003.

[24] Ates B, Sadoglu E. A quasi-2D exploration of optimum design settings for geotextile-reinforced sand in assistance with PIV analysis of failure mechanism. Geotext Geomembr 2023;vol. 51(3):418–36. https://doi.org/10.1016/j.geotexmem.2023.01.005.

[25] Guo X, Chen J, Xue J, Zhang Z. Centrifuge model and numerical studies of strip footing on reinforced transparent soils. Geosynth Int 2022;vol. 30(6):602–27. https://doi.org/10.1680/jgein.21.00120.

[26] Ateş B, Şadoğlu E. "Evaluation Bear Capacit increment Strip footing resting Soil Reinf wraparound Tech," 2023. https://doi.org/10.31462/icearc.2023.geo850.

[27] Ateş B, ŞADOĞLU E. "Vertical stress distribution in reinforced sandy soil in plane strain conditions,". Tek DERGI 2020;vol. 31(3). https://doi.org/10.18400/tekderg.449897.

[28] Wang J-Q, Zhang L-L, Xue J-F, Tang Y. Load-settlement response of shallow square footings on geogrid-reinforced sand under cyclic loading. Geotext Geomembr 2018;vol. 46(5):586–96. https://doi.org/10.1016/j.geotexmem.2018.04.009.

[29] Dai H, et al. Behavior study of shallowly buried large-span steel culverts by inclusion of geotextile reinforcements. Indian Geotech J 2024:1–10. https://doi.org/10.1007/s40098-024-00918-5.

[30] Beben D, Maleska T, Janda A, Nowacka J. The behaviour of shallow-buried corrugated steel plate bridge with RC Slab and EPS geofoam under static live loads. Transp Infrastruct Geotechnol 2023:1–21.

[31] Beben D, Stryczek A. Numerical analysis of corrugated steel plate bridge with reinforced concrete relieving slab. no 2016;vol. 22(5):585–96. https://doi.org/10.3846/13923730.2014.914092.
[32] Bakht B. "Live load response of a soil-steel structure with a relieving slab,". Transp Res Rec 1985;vol. 1008:1–7.
[33] Sanaeiha A, Rahimian M, Marefat MS. Field test of a large-span soil–steel bridge stiffened by concrete rings during backfilling. 06017002 J Bridg Eng 2017;vol. 22 (10). https://doi.org/10.1061/(asce)be.1943-5592.0001102.
[34] Bathurst RJ, Knight MA. Analysis of geocell reinforced-soil covers over large span conduits. Comput Geotech 1998;vol. 22(3–4):205–19. https://doi.org/10.1016/S0266-352X(98)00008-1.
[35] Wysokowski A. Durability of flexible steel corrugated shell structures-theory and practice. " *Arch Inst Civ Eng* 2017:347–60. https://doi.org/10.21008/j.1897-4007.2017.23.32.
[36] Wysokowski A. "Influence of single-layer geotextile reinforcement on load capacity of buried steel box structure based on laboratory full-scale tests,". Thin-Walled Struct 2021;vol. 159:107312.
[37] Fattah MY, Hassan WH, Rasheed SE. Behavior of flexible buried pipes under geocell reinforced subbase subjected to repeated loading. Int J Geotech Earthq Eng 2018;vol. 9(1):22–41.
[38] Xu C, Liang C, Shen P. Experimental and theoretical studies on the ultimate bearing capacity of geogrid-reinforced sand. Geotext Geomembr 2019;vol. 47(3):417–28. https://doi.org/10.1016/j.geotexmem.2019.01.003.
[39] Bartlett SF, Lingwall BN, Vaslestad J. Methods of protecting buried pipelines and culverts in transportation infrastructure using EPS geofoam. Geotext Geomembr 2015;vol. 43(5):450–61.
[40] N.R. EL-Sakhawy, H. Arafat, and A. Abd Allah, "Application of geogrids in a soil-steel culvert," Proc. XVII ECSMGE-2019, Reykjavik, Icel., 2019.
[41] Maleska T, Wysokowski A, Bęben D. Impact of reinforcement layer in soil-steel culvert on laboratory and numerical tests,". Int Sci Conf Environ Chall Civ Eng 2022:139–48.
[42] J. Vaslestad, L. Janusz, B. Bednarek, and Ł. Mielnik, "Instrumented full-scale test with geogird above the crown of corrugated steel box culvert," 2002.
[43] Hegde AM, Sitharam TG. Experimental and numerical studies on protection of buried pipelines and underground utilities using geocells. Geotext Geomembr 2015;vol. 43(5):372–81. https://doi.org/10.1016/j.geotexmem.2015.04.010.
[44] J.K. Jeyapalan and R.L. Lytton, "Stress reduction in flexible culverts due to overlays of geofabrics," in Proc. of 2nd International Conf. of Geotextiles, Las Vegas, USA, 1982, pp. 701–706.
[45] Palmeira EM, Bernal DF. Uplift resistance of buried pipes anchored with geosynthetics. Geosynth Int 2015;vol. 22(2):149–60. https://doi.org/10.1680/gein.15.00001.
[46] T. Zimmermann, A. Truty, A. Urbanski, and K. Podles, "ZSoil user manual," *Zace Serv. Switz.*, 2016.
[47] Machelski C, Sobótka M, Grosel S. Displacements of shell in soil-steel bridge subjected to moving load: determination using strain gauge measurements and numerical simulation. Stud Geotech Mech 2022;vol. 44(1). https://doi.org/10.2478/sgem-2021-0028.
[48] Łydżba D, Różański A, Sobótka M, Stefaniuk D, Chudy G, Wróblewski T. Mechanical behavior of soil-steel structure subjected to live loads and different water conditions. Arch Inst Inżynierii Lądowej 2017.
[49] Machelski C, Janusz L. Application of results of tests in developing a two-dimensional model for soil–steel railway bridges. Transp Res Rec 2017;vol. 2656 (1):53–60. https://doi.org/10.3141/2656-06.
[50] ViaCon Poland, "Catalogues English," 2022. ⟨https://viacon.pl/en/download⟩ (accessed Feb. 11, 2022).
[51] Alfaro MC, Blatz JA, Graham J. "Geosynthetic reinforcement for embankments over degrading discontinuous permafrost subjected to presstressing," (June) Lowl Technol Int 2006;vol. 8(1):47–54.
[52] C.S. Association, "CHBDC (Canadian Highway Bridge Design Code)," CAN/CSA-S6–14, 2019.
[53] Korusiewicz L, Kunecki B. Behaviour of the steel box-type culvert during backfilling. Arch Civ Mech Eng 2011;vol. 11(3):637–50. https://doi.org/10.1016/s1644-9665(12)60106-x.